ZITA MEDICAL MANAGEMENT

www.hsmc.gr/en/pharmakeftiki-journal/

PHARMAKEFTIKI, 37, 2S, 2025 | 235-238 RESEARCH

https://doi.org/10.60988/p.v37i2S.198

Antibacterial activity and structure properties of αFe_2O_3 nanoparticles synthesized by thermal precipitation method

Saba A. Habeeb[1], Asmaa H. Hammadi[2], Dhulfiqar A. Abed[3,*], Lena F. Hamza[4], Noor Z. Kbah[5]

[1]Department of Pharmaceutical Chemistry, College of Pharmacy, University of Babylon, Hillah, Iraq
[2]Department of Pharmaceutics, College of Pharmacy, University of Babylon, Hillah, Iraq
[3]Department of Pharmaceutical Chemistry, College of Pharmacy, Al Mustaqbal University, Hillah, Iraq
[4]Department of Pharmacology and Toxicology, College of Pharmacy, University of Babylon, Hillah, Iraq
[5]Department of Pharmaceutics, College of Pharmacy, Alzahraa University for Women, Karbala, Iraq

KEY WORDS:
αFe_2O_3 nanoparticles; thermal precipitation method; structural properties; antibacterial activity; *Staphylococcus aureus*

ARTICLE INFO:
Received: December 27, 2024
Revised: n/a
Accepted: January 06, 2025
Available online: October 10, 2025

*** CORRESPONDING AUTHOR:**
Dhulfiqar A. Abed, Department of Pharmaceutical Chemistry, College of Pharmacy, Al Mustaqbal University, Hillah, Iraq; e-mail: thulfigar.ali@uomus.edu.iq

ABSTRACT

In this study, alpha iron oxide (αFe_2O_3) nanoparticles (NPs) were successfully synthesized *via* a simple, cost-effective thermal precipitation method, with reaction parameters (such as temperature and alkalinity) systematically controlled in order to ensure high-quality outcomes. The structural and morphological properties of αFe_2O_3 NPs were characterized using Fourier-transform infrared spectroscopy (FT-IR), scanning electron microscopy (SEM), and X-ray diffraction (XRD). XRD analysis confirmed a hematite phase with an average crystallite size of 24 nm, while SEM imaging revealed NPs of defined morphology with an average particle size of approximately 57 nm. The antibacterial activity of αFe_2O_3 NPs against the Gram-positive bacterium *Staphylococcus aureus* was assessed using the agar well diffusion method. The NPs were tested at concentrations of 10, 15, 20, and 25 mg/mL, and their efficacy was compared to that of a standard antibiotic. The results demonstrated notable antibacterial activity at concentrations of 15 mg/mL and above, with clear zones of inhibition observed against *S. aureus.*

1. Introduction

Nanoparticles (NPs) are often regarded as "the wonders of modern medicine" due to their extraordinary biological and physical capabilities[1]. Iron oxides exhibit various crystalline phases, including those of hema-

PHARMAKEFTIKI, 37, 2S, 2025 | 235-238

tite (αFe_2O_3), akaganeite (βFe_2O_3), maghemite (γFe_2O_3), and magnetite (Fe_3O_4)[2]. Hematite, a magnetic, nontoxic, and corrosion-resistant compound, is especially valued for its wide range of applications in gas sensors, photocatalysis, lithium- and sodium-ion batteries, magnetic materials, supercapacitors, optical devices, and biomedical technologies[3].

Metal oxide NPs play a critical role across chemistry, materials science, and biology. Owing to their electronic properties, they are well-suited for use in sensors and conductors. Their suitability for medical and pharmaceutical applications (including controlled drug release, diagnostics, and wound healing) is attributed to their distinctive physicochemical properties and antibacterial activity. These features suggest that metal NPs may serve as effective carriers for targeting bacterial biofilms and multidrug-resistant infections when formulated with appropriate antimicrobial payloads.

Metal oxide NPs exhibit multiple mechanisms of antibacterial action. Key among them are their size and morphology, which offer a high surface-to-volume ratio and thereby enhance interaction with bacterial cells. Mechanisms include disruption of bacterial cell walls, induction of oxidative stress, and release of metal ions. These features make metal oxide NPs particularly effective at reducing the likelihood of bacterial resistance. Moreover, their ability to generate reactive oxygen species (ROS) under specific conditions enhances their antimicrobial activity. An additional antibacterial mechanism involves the release of heavy metal ions[4].

This study evaluates the antibacterial activity of αFe_2O_3 NPs against *Staphylococcus aureus* over a concentration range of 5, 10, 15, and 25 mg/L. The optimum inhibitory concentration was found to be 25 mg/L.

2. Methodology

2.1. Synthesis of αFe_2O_3 NPs

Pure αFe_2O_3 NPs were synthesized using ferric chloride hexahydrate ($FeCl_3 \cdot 6H_2O$). Specifically, 4 g (0.05 M) of $FeCl_3 \cdot 6H_2O$ was dissolved in 100 mL of distilled water and stirred magnetically for 30 min at 70°C. To adjust the pH to 11, a precipitating agent – 50 mL of NaOH (2 M) – was gradually added under continuous stirring for 3 h. The resultant precipitate was collected and centrifuged at 6,000 rpm, followed by repeated rinsing with distilled water to eliminate residual chlorides. The precipitate was dried at 80°C, and the sample – designated as "Fe_2O_3 500°C" – was calcined for 4 h at 500°C[5].

2.2. Antibacterial activity assay

The antibacterial efficacy of αFe_2O_3 NPs against Gram-positive *Staphylococcus aureus* was assessed *via* the agar well diffusion method. Comparative analysis was performed against established antibiotic controls. Test organisms were cultured in nutrient broth at 37°C for 24 h. Post incubation, the inoculum was evenly spread onto Mueller-Hinton agar plates using sterile swabs. Wells of 6-mm diameter were created using a sterile cork borer, and 100 µL of NP suspensions (10, 15, 20, and 25 mg/mL in distilled water) were added to the wells. Plates were incubated at 37°C for 24 h, and antibacterial activity was evaluated by measuring the diameter of the inhibition zones (in mm).

3. Results and Discussion

X-ray diffraction (XRD) analysis confirmed the crystal structure and phase composition of the αFe_2O_3 NPs. As shown in Figure 1A, all peaks corresponded well to the hexagonal hematite phase of αFe_2O_3 (JCPDS card no. 33-0664). The average crystallite size of 24 nm was calculated using the Debye-Scherrer formula[7], and powder formation may reflect grain coalescence.

Scanning electron microscopy analysis (Figure 1B) revealed particles of uneven size and morphology, largely tending toward distorted spherical forms with an average diameter of approximately 57 nm. Fourier-transform infrared (FT-IR) spectroscopy (Figure 1C) exhibited prominent absorption bands at 530 cm^{-1} and 4850 cm^{-1}. A weaker Fe–O stretching vibration peak appeared at 1515.5 cm^{-1}, consistent with commercial αFe_2O_3 spectra[8].

Figure 1D illustrates the inhibition zones produced

PHARMAKEFTIKI, 37, 2S, 2025 | 235-238

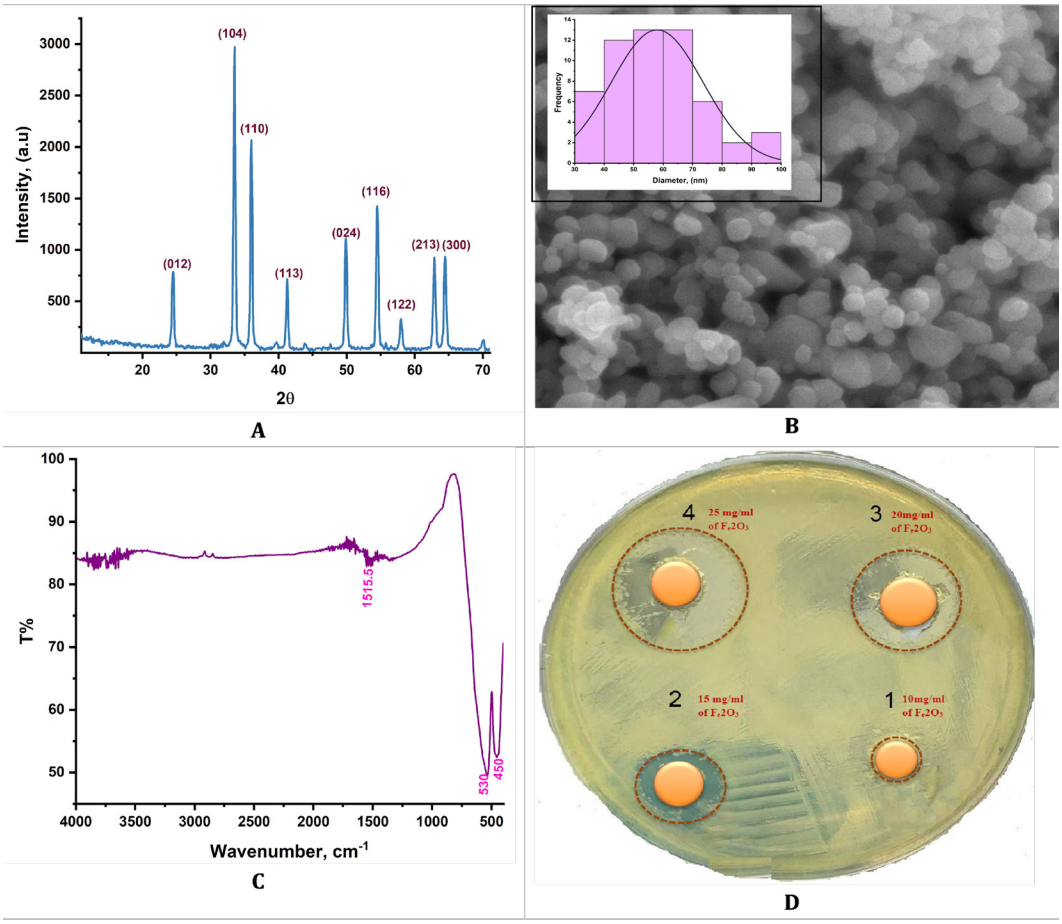

Figure 1. *Structural characterization and antibacterial assessment of alpha iron oxide (αFe_2O_3) nanoparticles (NPs). (A): X-ray diffraction patterns confirming the hematite phase of αFe_2O_3 NPs. (B): Scanning electron microscopy image depicting the morphology and particle size distribution of αFe_2O_3 NPs. (C): Fourier-transform infrared spectra of αFe_2O_3 NPs highlighting key vibrational bands. (D): Zones of inhibition illustrating the antibacterial efficacy of αFe_2O_3 NPs against Staphylococcus aureus via the agar well diffusion method.*

by increasing concentrations (10, 15, 20, and 25 mg/mL) of αFe_2O_3 NPs against *S. aureus*. Antibacterial activity increased proportionally with concentration, with significant inhibition observed at 15 mg/mL and above.

The antimicrobial mechanism of αFe_2O_3 NPs primarily involves the generation of ROS under oxidative stress. These ROS induce biomolecular damage (including DNA fragmentation, protein oxidation, and lipid peroxidation), ultimately leading to bacterial cell death. Additionally, the release of positively charged metal ions may disrupt membrane integrity and hinder DNA replication *via* electrostatic interactions with negatively charged bacterial surfaces.

Zones of inhibition reflect the NPs' antibacterial efficacy, yet several factors influence these measurements. These include NP concentration, incubation time, bacterial strain, diffusion rate through agar, and particle–cell wall interaction. Synergistic or antagonistic effects within the agar medium also modulate antimicrobial performance. Thus, inhibition zone measurements alone should not be used in order to quantify antibacterial potency; rather, they must be interpreted in the context of these complex factors[8,9].

PHARMAKEFTIKI, 37, 2S, 2025 | 235-238

4. Conclusion

The herein assessed αFe_2O_3 NPs were successfully synthesized *via* a thermal precipitation method. XRD confirmed a hexagonal hematite phase, with an average particle size of 57 nm. Antibacterial testing demonstrated pronounced activity against *Staphylococcus aureus*, with efficacy increasing in a dose-dependent manner. These findings suggest that αFe_2O_3 NPs may serve as effective nanocarriers for enhancing the performance of antimicrobial agents.

Acknowledgements
None.

Conflicts of interest

None exist.

ORCIDs

0000-0001-8044-7969 (S.A. Habeeb); 0000-0003-2228-1416 (A.H. Hammadi); 0000-0002-6004-9602 (D.A. Abed); 0000-0001-7071-3442 (L.F. Hamza); 0009-0004-5600-434X (N.Z. Kbah)

References

1. Al-Assaly R., Habeeb S.A., Hammadi A.H., Al-Jibouri L.F., Hameed R., Al-Nafiey A. Antimicrobial performance and instrumental analysis for hexagonal ZnO NPs biosynthesized via *Ziziphus* leaf extract. *Oxf. Open Mater. Sci.* 4(1), itae011, 2024. DOI: 10.1093/oxfmat/itae011
2. Suman C.S., Kumar A., Kumar P. Zn doped α-Fe_2O_3: an efficient material for UV driven photocatalysis and electrical conductivity. *Crystals* 10, 273, 2020. DOI: 10.3390/cryst10040273
3. Liu J., Yang H., Xue X. Preparation of different shaped α-Fe_2O_3 nanoparticles with large particles of iron oxide red. *CrystEngComm* 21(7), 1097–1101, 2019. DOI: 10.1039/c8ce01920g
4. Naushin F., Sen S., Kumar M., Bairagi H., Maiti S., Bhattacharya J., *et al.* Structural and surface properties of pH-varied Fe_2O_3 nanoparticles: correlation with antibacterial properties. *ACS Omega* 9(1), 464–473, 2023. DOI: 10.1021/acsomega.3c05930
5. Valášková M., Tokarský J., Pavlovský J., Prostějovský T., Kočí K. α-Fe_2O_3 nanoparticles/vermiculite clay material: structural, optical and photocatalytic properties. *Materials (Basel)* 12(11), 1880, 2019. DOI: 10.3390/ma12111880
6. Hooda R., Sharma M. Green synthesis, characterization and antibacterial activity of iron oxide nanoparticles. *Plant Arch.* 20(1), 1196–1200, 2020.
7. Habeeb S.A., Zinatizadeh A.A., Zangeneh H. Photocatalytic decolorization of direct red16 from an aqueous solution using B-ZnO/TiO_2 nano photocatalyst: synthesis, characterization, process modeling, and optimization. *Water* 15, 1203, 2023. DOI: 10.3390/w15061203
8. Han Q., Zhang D., Guo J., Zhu B., Huang W., Zhang S. Improved catalytic performance of Au/α-Fe_2O_3-like-worm catalyst for low temperature CO oxidation. *Nanomaterials (Basel)* 9(8), 1118, 2019. doi: 10.3390/nano9081118
9. Alnehia A., Hadi M., Alnahari H., Al-Sharabi A. Optical, structural and antibacterial properties of phase heterostructured Fe_2O_3-CuO-$CuFe_2O_4$ nanocomposite. *Sci. Rep.* 14(1), 14392, 2024. DOI: 10.1038/s41598-024-64090-9

HOW TO CITE:
Habeeb S.A., Hammadi A.H., Abed D.A., Hamza L.F., Kbah N.Z. Antibacterial activity and structure properties of αFe_2O_3 nanoparticles synthesized by thermal precipitation method. *Pharmakeftiki* 37(2s), 235-238, 2025. https://doi.org/10.60988/p.v37i2S.198